Energy-Aware Resource Allocation and Trajectory Design for UAV-Enabled ISAC

Ata Khalili*, Atefeh Rezaei†, Dongfang Xu*, and Robert Schober*

*Friedrich-Alexander-University Erlangen-Nurnberg, Germany;†Technical University of Berlin, Germany

Abstract

In this paper, we investigate joint resource allocation and trajectory design for multi-user multi-target unmanned aerial vehicle (UAV)-enabled integrated sensing and communication (ISAC). To improve sensing accuracy, the UAV is forced to hover during sensing. In particular, we jointly optimize the two-dimensional trajectory, velocity, downlink information and sensing beamformers, and sensing indicator to minimize the average power consumption of a fixed-altitude UAV, while considering the quality of service of the communication users and the sensing tasks. To tackle the resulting non-convex mixed integer non-linear program (MINLP), we exploit semidefinite relaxation, the big-M method, and successive convex approximation to develop an alternating optimization-based algorithm. Our simulation results demonstrate the significant power savings enabled by the proposed scheme compared to two baseline schemes employing heuristic trajectories.

I. Introduction

Integrated sensing and communication (ISAC) has lately drawn significant attention as a promising technology to increase the spectrum efficiency and enable the sharing of the physical infrastructure for sensing and communications in sixth-generation (6G) wireless communication systems [1]. In this regard, the authors of [2], [3] studied transmit beamforming for ISAC systems, where a least-squares problem was formulated to obtain the ideal beampattern for sensing while guaranteeing a required signal-to-interference-plus-noise ratio (SINR) of the communication users. However, these works considered terrestrial ISAC systems which are typically impaired by surrounding obstacles and scatters on the ground blocking the line of sight (LoS) to the sensing targets.

On the other hand, unmanned aerial vehicle (UAV)-aided wireless communication has drawn significant attention as a result of its simple deployment and favorable channel characteristics [4],

[5]. In fact, UAVs can facilitate LoS links which are also desirable for sensing. This is because target detection and parameter estimation require LoS links between the sensing transceivers and the sensing targets. Furthermore, due to their high maneuverability, UAVs can significantly reduce the typically high sensing powers as they can get close to the targets [6]. Despite these promising features, only few works in the existing literature have studied UAV-enabled ISAC [7]–[10]. The authors in [7] optimized the trajectory, transmit beamforming, and radar signals of a UAV-enabled ISAC system to improve the communication data rate while ensuring a required sensing beampattern gain. In [8], a periodic sensing and communication scheme for UAV-enabled ISAC systems was introduced and the achievable rate was maximized by jointly optimizing the UAV's trajectory, transmit precoder, and sensing start time subject to sensing frequency and beampattern gain constraints. Besides, in [9], user association, sensing time selection, beamforming, and the UAV trajectory were jointly optimized to boost the total achievable data rate of an UAV-based ISAC system. The authors in [10] proposed a novel integrated sensing, jamming, and communication framework for UAV-enabled downlink communications to maximize the number of securely served users while considering a tracking performance constraint. Yet, the authors of [7]–[10] focus only on beampattern gain optimization for target sensing and do not take into account the sidelobes of the beams which waste energy and may cause unwanted interference [2], [3]. Besides, sensing was performed while the UAV was moving, which may degrade the sensing accuracy [11]. Hence, in this paper, we enforce that sensing is performed only when the UAV is hovering. First, during hovering, the effect of UAV jittering is smaller as compared to when the UAV moves which results in a better sensing performance [12]. Second, when the UAV hovers exactly above the target the predetermined beampattern can be easily designed as the beampattern is fixed and does not need to be continuously adjusted according to the UAV's flight path which reduces the design complexity significantly. In this paper, we optimize the average power consumption of the UAV taking into account the quality of service (QoS) requirements of the communication users and the sensing tasks. The main contributions of this paper can be summarized as follows:

- We investigate the joint resource allocation and trajectory design for an UAV-enabled ISAC system to minimize the average power consumption of the UAV. To this end, we formulate an optimization problem where also the time when the UAV hovers for sensing is subjected to optimization which leads to a non-convex mixed integer non-linear program (MINLP).

Fig. 1: Joint communication and sensing in UAV-assisted network comprising $E = 2$ sensing targets and $K = 2$ communication users.

- We develop an alternative optimization (AO) based resource allocation algorithm to solve the optimization problem. In particular, we obtain a low-complexity sub-optimal solution for the formulated highly non-convex MINLP by exploiting semi-definite relaxation, the big-M method, and successive convex approximation (SCA).
- Simulation results demonstrate the superiority of our proposed resource allocation algorithm compared to two baseline schemes in terms of average power consumption. Besides, we also show that the proposed algorithm successfully forces the UAV to perform sensing while hovering above the target.

Notations: In this paper, matrices and vectors are denoted by boldface capital letters $\mathbf{A}$ and lower case letters $\mathbf{a}$, respectively. $\mathbf{A}^T$, $\mathbf{A}^H$, Rank$(\mathbf{A})$, and Tr$(\mathbf{A})$ are the transpose, Hermitian conjugate transpose, rank, and trace of matrix $\mathbf{A}$, respectively. $\mathbf{A} \succeq \mathbf{0}$ denotes a positive semidefinite matrix. $\mathbf{I}_N$ is the N-by-N identity matrix. The absolute value of a complex scalar and the Euclidean norm of a complex vector are denoted by $|\cdot|$ and $\|\cdot\|$, respectively. $\mathcal{CN}(\boldsymbol{\mu}, \mathbf{C})$ represents the circularly symmetric complex Gaussian (CSCG) distribution with mean $\boldsymbol{\mu}$ and covariance matrix $\mathbf{C}$. Finally, $\mathbb{C}^{M\times N}$ represents an $M \times N$ dimensional complex matrix and $\nabla_{\mathbf{x}}$ is the gradient with respect to $\mathbf{x}$.

II. System Model

In this paper, we consider an UAV-assisted ISAC system that provides downlink communication services for K communication users and senses E potential targets as shown in Fig. 1. The UAV's total flying time T is divided into N time slots of duration $\delta_t = \frac{T}{N}$. Each time slot is assumed to be sufficiently small, such that the location of the UAV can be assumed to be approximately constant during a time slot which facilitates the trajectory and beamforming design for ISAC. We adopt a three-dimensional (3D) Cartesian coordinate system where the horizontal location of the UAV and the k^{th} communication user in time slot n are denoted by $\mathbf{q}[n] = \big[q_x[n], q_y[n]\big]^T$ and $\mathbf{d}_k = \big[d_{x_k}, d_{y_k}\big]^T$, respectively. Moreover, it is assumed that the UAV flies in the $x-y$ plane at fixed altitude H subject to air traffic control. The UAV is equipped with a uniform linear array (ULA) with M antennas and transmits simultaneously information signals $c_k[n]$, $c_k \sim \mathcal{CN}(0,1)$, $k \in \{1,...,K\}$, to K communication users. Hence, the baseband transmit signal of the UAV in time slot n can be expressed as follows

$$\mathbf{x}[n] = \sum_{k=1}^{K} \mathbf{w}_k[n] c_k[n], \tag{1}$$

where $\mathbf{w}_k[n] \in \mathbb{C}^{M\times 1}$ denotes the transmit beamforming vector for user k.

A. ISAC Frame Structure

The proposed frame structure for UAV-ISAC is shown in Fig. 2. The UAV can communicate with the communication users in all time slots. However, the UAV can use only a maximum of $N_s^{\max}$ time slots for sensing. During sensing at most one target is sensed at a time to maximize the sensing performance by focusing the beampattern on the target. However, when sensing is performed is part of the optimization. To this end, we define $\alpha_{e,n}$ as the sensing indicator for target e, $e \in \{1,...,E\}$. In particular, if $\alpha_{e,n} = 1$, target e is sensed in the n-th time slot, during which the UAV is forced to hover above the target; otherwise, $\alpha_{e,n} = 0$.

B. Radar and Communication Models

The location of the potential target on the ground is denoted by $\mathbf{d}_e = \big[d_{x_e}, d_{y_e}\big]^T \in \mathbb{R}^{2\times 1}$. The value of $\mathbf{d}_e$, $e \in \{1,...,E\}$, is predetermined based on the specific sensing tasks[1]. The UAV emits

[1]The value of $\mathbf{d}_e$ could be set based on an estimated location for target tracking or it could be a fixed location in the region of interest for target detection [8], [9].

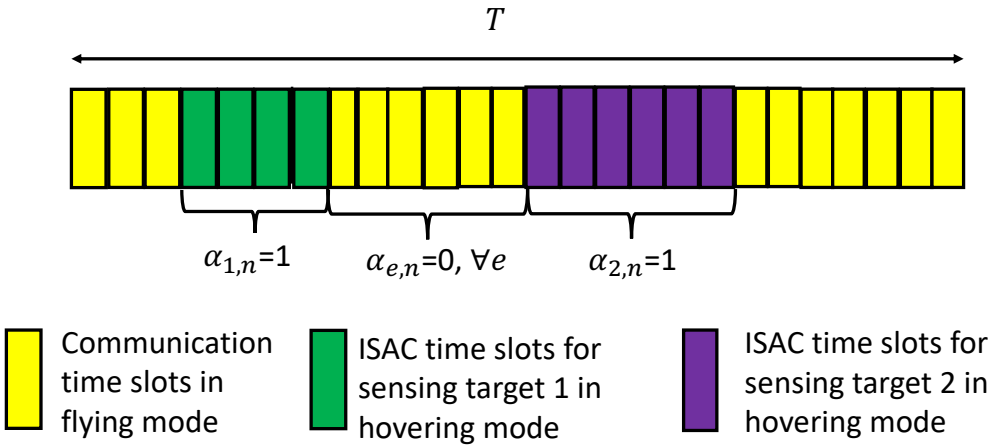

Fig. 2: Proposed ISAC frame structure where T is the total flying time.

.

a narrow beam towards the direction of the target to obtain the information of the targets. Here, the communication signals are also exploited for sensing. The transmit beampattern gain from the UAV in the direction of target e is given by $\mathcal{P}(\mathbf{w}_k, \mathbf{q}[n], \mathbf{d}_e) = \mathbf{a}^H(\mathbf{q}[n], \mathbf{d}_e) \left(\sum_{k=1}^{K} \mathbf{w}_k[n]\mathbf{w}_k^H[n] \right) \mathbf{a}(\mathbf{q}[n], \mathbf{d}_e)$, where

$$\mathbf{a}(\mathbf{q}[n], \mathbf{d}_e) = \left[1, e^{j2\pi \frac{\hat{d}}{\lambda} \cos(\theta(\mathbf{q}[n], \mathbf{d}_e))}, ..., e^{j2\pi \frac{\hat{d}}{\lambda}(M-1) \cos(\theta(\mathbf{q}[n], \mathbf{d}_e))}\right]^T$$

is the steering vector, $\theta(\mathbf{q}[n], \mathbf{d}_e) = \arccos\left(\frac{H}{\sqrt{\|\mathbf{q}[n]-\mathbf{d}_e\|^2+H^2}}\right)$ is the angle of departure corresponding to target e, λ is the carrier wavelength, and $\hat{d}$ denotes the spacing between two adjacent UAV antennas.

Next, the echo signal received at the UAV in time slot n is given by $\mathbf{r}_e[n] = \mathbf{H}_e[n] \left(\sum_{k=1}^{K} \mathbf{w}_k[n] s_k[n] \right) + \mathbf{z}[n]$, where $\mathbf{z} \sim \mathcal{CN}(\mathbf{0}, \sigma_e^2 \mathbf{I}_M)$ is the received additive white Gaussian noise (AWGN) at the UAV and $\mathbf{H}_e[n]$ is the round-trip channel matrix, which is given by $\mathbf{H}_e[n] = \frac{\epsilon_e[n]\beta_0}{2\Psi_e[n]} \mathbf{a}(\mathbf{q}[n], \mathbf{d}_e)\mathbf{a}^H(\mathbf{q}[n], \mathbf{d}_e)$, where β_0 denotes the channel power gain at the reference distance of $d_0 = 1$ m and $\Psi_e[n] = \sqrt{\|\mathbf{q}[n] - \mathbf{d}_e\|^2 + H^2}$. Moreover, $\epsilon_e[n] = \sqrt{\frac{\vartheta_e}{4\pi\Psi_e^2[n]}}$ denotes the reflection coefficient of target e in time slot n, and ϑ_e is the radar cross-section of target e [13]. To achieve adequate sensing performance, we require the accumulated sensing SNR of target e to be higher than a preset minimum threshold as $\Gamma_e \triangleq \sum_{n=1}^{N} \alpha_{e,n} \frac{\vartheta_e \beta_0^2 \mathbf{a}^H(\mathbf{q}[n], \mathbf{d}_e) \left(\sum_{k=1}^{K} \mathbf{w}_k[n]\mathbf{w}_k^H[n] \right) \mathbf{a}(\mathbf{q}[n], \mathbf{d}_e)}{16\pi\Psi_e^4[n]\sigma_e^2} \geqslant \text{SNR}_e^{\text{th}}$, where SNR_e^{th} is the minimum SNR

TABLE I: Parameters in the power consumption model [14].

Notations	Definitions
$\Omega = 300$	Blade angular velocity in radians/second
$r = 0.4$	Rotor radius in meter
$\rho = 1.225$	Air density in $\mathrm{kg/m^3}$
$s = 0.05$	Rotor solidity in $\mathrm{m^3}$
$A_{\mathrm{r}} = 0.503$	Rotor disc area in $\mathrm{m^2}$
$P_o = 80$	Blade profile power during hovering in Watt
$P_i = 88.6$	Induced power during hovering in Watt
$v_0 = 4.03$	Mean rotor induced velocity in forward flight in m/s
$r_0 = 0.6$	Fuselage drag ratio

required at the UAV for sensing target e. The channel vector between the UAV and user k is denoted by $\mathbf{h}_k$, and given by $\mathbf{h}_k[n] = \frac{\beta_0 \mathbf{a}(\mathbf{q}[n],\mathbf{d}_k[n])}{\sqrt{\|\mathbf{q}[n]-\mathbf{d}_k[n]\|^2+H^2}}$, based on the free space channel model. Then, the received signal at user k can be written as $y_k[n] = \mathbf{h}_k^H[n]\left(\sum_{k=1}^K \mathbf{w}_k[n]s_k[n]\right) + z_k[n]$, where $n_k \sim \mathcal{CN}(0,\sigma_k^2)$ is the AWGN at user k. Consequently, the received SINR of user k in time slot n is given by

$$\gamma_k[n] = \frac{\left|\mathbf{h}_k^H[n]\mathbf{w}_k[n]\right|^2}{\sum_{i\neq k}\left|\mathbf{h}_k^H[n]\mathbf{w}_i[n]\right|^2 + \sigma_k^2}. \tag{2}$$

C. Power Consumption Model

The propulsion power consumption depends on the flying mode of the UAV [5], [14]. In particular, the aerodynamic power consumption for rotary-wing UAVs is a function of its flight velocity $\mathbf{v}[n] \in \mathcal{R}^{2\times 1}$ [14]. The total power consumption in time slot n can be written as $P(\mathbf{v}[n]) = \sum_{e=1}^E \alpha_{e,n} P_{\text{hover}}[n] + (1-\sum_{e=1}^E \alpha_{e,n}) P_{\text{fly}}(\mathbf{v}[n])$, where $P_{\text{hover}} = P_o + P_i$ and P_{fly}=$P_o\left(\frac{3\|\mathbf{v}[n]\|^2}{\Omega^2 r^2}\right) + P_i\left[\left(\sqrt{1+\frac{\|\mathbf{v}[n]\|^4}{4v_0^4}} - \frac{\|\mathbf{v}[n]\|^2}{2v_0^2}\right)^{1/2} - 1\right] + \frac{1}{2} r_0 \rho s A_{\mathrm{r}} \|\mathbf{v}[n]\|^3$. The parameters of the power consumption model are summarized in Table I [14].

III. Problem Formulation

In this paper, we aim to minimize the average power consumption of the UAV by jointly optimizing the beamforming for information transmission and sensing, the time slots when the UAV hovers above the target for sensing, $\alpha_{e,n}$, the UAV trajectory ($\mathbf{q}$), and the velocity of the UAV ($\mathbf{v}$), while guaranteeing the QoS of the communication users and the sensing targets. As a result, the optimization problem is mathematically formulated as follows:

transmit beamforming energy

$$\mathcal{P}_1: \min_{\mathbf{\Xi}} \mathcal{O} \triangleq \frac{1}{N}\sum_{n=1}^{N}\Bigg(\sum_{k=1}^{K}\|\mathbf{w}_k[n]\|^2+ \sum_{e=1}^{E}\alpha_{e,n}P_{\text{hover}}[n]+(1-\sum_{e=1}^{E}\alpha_{e,n})P_{\text{fly}}(\mathbf{v}[n])\Bigg)$$

$$\text{s.t.}\quad \text{C1}: \sum_{k=1}^{K}\|\mathbf{w}_k[n]\|^2 \leqslant P_{\max}, \quad \text{for all n?} \quad \text{hardware limitation}$$

$$\text{C2}: \frac{1}{N}\sum_{n=1}^{N}\log_2(1+\gamma_k[n]) \geqslant R_{\min}^k, \forall k, \quad \text{average data rate for each user}$$

$$\text{C3}: \alpha_{e,n}\Big\|\sum_{k=1}^{K}\mathbf{w}_k[n]\mathbf{w}_k^H[n]-\mathbf{R}_d\Big\|_F^2 \leqslant \epsilon, \quad \text{C4}: \Gamma_e \geqslant \text{SNR}_{\text{e}}^{\text{th}}, \quad \text{SNR of sensing echo}$$

$$\text{C5}: \sum_{e=1}^{E}\alpha_{e,n} \leqslant 1, \forall n, \quad \text{C6}: \sum_{n=1}^{N}\alpha_{e,n} \leqslant N_s^{\max}, \forall e$$

only one target at a time — sensing time slots limited

$$\text{C7}: \sum_{e=1}^{E}\alpha_{e,n}\|\mathbf{q}[n]-\mathbf{d}_e\|^2 \leqslant D, \quad \text{maximum distance to sensing target}$$

$$\text{C8}: \mathbf{q}[n+1]=\mathbf{q}[n]+(1-\sum_{e=1}^{E}\alpha_{e,n})\mathbf{v}[n]\delta_t, \forall n, e, \quad \text{trajectory dynamics}$$

$$\text{C9}: \|\mathbf{v}[n+1]-\mathbf{v}[n]\| \leqslant a_{\max}\delta_t, \forall n, \quad \text{limited acceleration}$$

$$\text{C10}: \|\mathbf{v}[n]\| \leqslant (1-\sum_{e=1}^{E}\alpha_{e,n})v_{\max}, \forall n, \quad \text{limited velocity}$$

$$\text{C11}: \alpha_{e,n} \in \{0,1\}, \forall e, n. \quad \text{either sense or not} \tag{3}$$

In (3), $\mathbf{\Xi}=\{\mathbf{w}_k[n], \mathbf{q}[n], \mathbf{v}[n], \alpha_{e,n}\}$ is the set of optimization variables. C1 limits the transmit power of the UAV, where $P_{\max}$ is the maximum transmit power. C2 guarantees that the average achievable data rate of the communication users does not fall below the minimum data rate $R_{\min}^k$. C3 ensures that the difference between the desired radar beampattern and the actual beampattern of the transmitted signal does not exceed a predefined threshold. In particular, the predesigned highly-directional sensing beampattern is characterized by the covariance matrix of the desired waveform, i.e., $\mathbf{R}_d$ [2]. C4 ensures the accumulated SNR of the reflected signal at the UAV does not fall below a threshold. C5 indicates that at most one target can be sensed in a time slot. C6 limits the maximum number of time slots for sensing to $N_s^{\max}$. C7 ensures the horizontal

[2]This constraint can be used to synthesize a focused beam with small sidelobes for sensing minimizing interference and clutter. Note that $\mathbf{R}_d$ is independent of the trajectory as C7 ensures the UAV always hovers above the target for sensing.

distance between the UAV and the target is smaller than D. For smaller D, the UAV will hover above the target during sensing. C8 describes the evolution of the trajectory of the UAV based on its flight velocity. Furthermore, C9 and C10 limit the maximum acceleration and velocity of the UAV to $a_{\max}$ and $v_{\max}$, respectively. Finally, C11 ensures that the sensing indicator is an integer variable.

IV. Solution of the Optimization Problem

Optimization problem $\mathcal{P}_1$ is non-convex due to the coupling between the variables and the non-convexity of constraints $\text{C2}-\text{C4}, \text{C7}, \text{C8}$, and of the power consumption of the UAV in the objective function. In general, it is very challenging to find the optimal solution of problem $\mathcal{P}_1$ in polynomial time. Therefore, we propose an iterative algorithm based on the AO approach. In particular, we first optimize the beamforming matrices and the sensing indicator at the UAV, and then we jointly optimize the trajectory and velocity of the UAV.

A. Beamforming and Sensing Indicator Optimization

First, we assume that the position and velocity of the UAV are fixed and we aim to optimize the beamformers for communication and sensing. To do so, we employ semidefinite programming (SDP) and define $\mathbf{W}_k = \mathbf{w}_k \mathbf{w}_k^H$, where $\mathbf{W}_k \succeq 0$ and $\text{Rank}(\mathbf{W}_k) \leqslant 1$. One obstacle for solving optimization problem $\mathcal{P}_1$ is the coupling of $\alpha_{e,n}$ with $\mathbf{W}_k[n]$ in C3 and C4. In order to overcome this difficulty, we adopt the big-M formulation. In particular, we define the new optimization variable $\tilde{\mathbf{W}}_{k,e}[n] = \alpha_{e,n} \mathbf{W}_k[n]$ and add the following additional constraints to the optimization problem:

$$\text{C12}: \tilde{\mathbf{W}}_{k,e}[n] \preceq \alpha_{e,n}\ P_{\max}\ \mathbf{I}_M, \quad \text{enforce Pmax during sensing?} \tag{4}$$

$$\text{C13}: \tilde{\mathbf{W}}_{k,e}[n] \preceq \mathbf{W}_{k,e}[n],\ \ \text{C14}: \tilde{\mathbf{W}}_{k,e}[n] \succeq \mathbf{0}, \tag{5}$$

$$\text{C15}: \tilde{\mathbf{W}}_{k,e}[n] \succeq \mathbf{W}_{k,e}[n] - (1-\alpha_{e,n})\ P_{\max}\ \mathbf{I}_M. \tag{6}$$

all needed? what exactly do they enforce?

Besides, we introduce a set of auxiliary optimization variables $\mu_k[n]$ to bound the SINR from below [15]

$$0 \leqslant \mu_k[n] \leqslant \frac{\text{Tr}\big(\mathbf{W}_k[n]\mathbf{H}_k[n]\big)}{\sum_{i\neq k} \text{Tr}\big(\mathbf{W}_i[n]\mathbf{H}_k[n]\big) + \sigma_k^2}, \tag{7}$$

Total power received for com user k

SINR

interference + noise power

where $\mathbf{H}_k[n] = \mathbf{h}_k[n]\mathbf{h}_k^H[n]$. However, (7) is still non-convex. To overcome this issue, by introducing auxiliary variable $\phi_k[n]$, we can rewrite C2 as follows:

Total power received for com user k

$$\text{C2a}: \text{Tr}\big(\mathbf{W}_k[n]\mathbf{H}_k[n]\big) \geqslant \mu_k[n]\phi_k[n], \tag{8}$$

auxiliary variables

$$\text{C2b}: \sum_{i\neq k} \text{Tr}\big(\mathbf{W}_i[n]\mathbf{H}_k[n]\big) \leqslant \phi_k[n]. \tag{9}$$

interference power

The left-hand side of (8) is convex. However, the right-hand side is a product of two terms and not convex. Nevertheless, we can rewrite the product of the two terms as

$$\mu_k[n]\phi_k[n] = 0.5\big(\mu_k[n] + \phi_k[n]\big)^2 - 0.5\big(\mu_k^2[n] + \phi_k^2[n]\big). \tag{10}$$

Note that (10) is a difference of concave (DC) functions [16]. As a result, the first-order Taylor approximation can be adopted to obtain a concave function and $\mu_k[n]\phi_k[n]$ can be bounded as follows:

$$\begin{aligned}\mu_k[n]\phi_k[n] \geqslant\ & 0.5\big(\mu_k'[n] + \phi_k[n]\big)^2 - \\ & \mu_k^{(t)}\big(\mu_k[n] - \phi_k^{(t)}[n]\big) - \phi_k^{(t)}[n]\big(\phi_k[n] - \phi_k^{(t)}[n]\big) \triangleq \nu_k[n]\end{aligned} \tag{11}$$

where t denotes iteration index for SCA. Next, we relax the integer variable to a continuous one and rewrite C11 as follows:

$$\text{C11a}: 0 \leqslant \alpha_{e,n} \leqslant 1,\ \ \text{C11b}: \sum_{e=1}^{E}\sum_{n=1}^{N} \alpha_{e,n} - \alpha_{e,n}^2 \leqslant 0. \tag{12}$$

Constraint C11b is a DC function and we use first-order Taylor approximation to convert the non-convex constraint to the following convex constraint

$$\overline{\text{C11b}}: \sum_{e=1}^{E}\sum_{n=1}^{N} \big(\alpha_{e,n} - 2\alpha_{e,n}^{(t)}(\alpha_{e,n} - \alpha_{e,n}^{(t)})\big) \leqslant 0. \tag{13}$$

Now, we introduce a penalty factor τ to add $\overline{\text{C11b}}$ to the objective function. Thus, optimization problem $\mathcal{P}_1$ can be restated as follows

$$\begin{aligned}\mathcal{P}_2: \min_{\tilde{\mathbf{\Xi}}}\ & \frac{1}{N}\sum_{n=1}^{N}\Bigg(\sum_{k=1}^{K}\text{Tr}(\mathbf{W}_k[n]) + \\ & \sum_{e=1}^{E}\alpha_{e,n}P_{\text{hover}}[n] + (1 - \sum_{e=1}^{E}\alpha_{e,n})P_{\text{fly}}(\mathbf{v}[n])\Bigg) + \\ & \tau\Bigg(\sum_{e=1}^{E}\sum_{n=1}^{N}\big(\alpha_{e,n} - 2\alpha_{e,n}^{(t)}(\alpha_{e,n} - \alpha_{e,n}^{(t)})\big)\Bigg) \\ \text{s.t.}\ \ & \text{C1}: \sum_{k=1}^{K}\text{Tr}(\mathbf{W}_k[n]) \leqslant P_{\max},\end{aligned}$$

$$\text{C2c}: \frac{1}{N}\sum_{n=1}^{N}\log_2(1+\mu_k[n]) \geqslant R_{\min}^k,$$

$$\overline{\text{C2a}}: \text{Tr}\big(\mathbf{W}_k[n]\mathbf{H}_k[n]\big) \geqslant \nu_k[n],\ \text{C2b},$$

sinr * interference power

dropped $\text{C16}: \text{Rank}(\mathbf{W}_k) \leqslant 1,\ \text{C3}-\text{C8},\ \text{C11a}, \text{C10}-\text{C15},$ (14)

where $\widetilde{\boldsymbol{\Xi}} = \{\mathbf{W}_k[n], \tilde{\mathbf{W}}_{k,e}[n], \alpha_{e,n}, \mu_k[n], \phi_k[n]\}$ is the new set of optimization variables. Here, penalty factor τ can be used to penalize the objective function to enforce binary values for $\alpha_{e,n}$. Now, by dropping the rank-one constraint on $\mathbf{W}_k[n]$ and adopting SDP relaxation, problem $\mathcal{P}_2$ becomes a convex optimization problem and can be efficiently solved by CVX. The tightness of the SDP relaxation can be proved following similar steps as in [17, Appendix A]. We omit the proof here due to space constraints.

B. Trajectory Design and Velocity Optimization

Now, we tackle the design of the trajectory and velocity of the UAV for given beamforming matrices and sensing indicators. Let us first define slack variable $s_k[n] = \|\mathbf{q}[n] - \mathbf{d}_k[n]\|^2 + H^2$. Next, we handle the non-convexity of the data rate constraint in C2. By introducing new auxiliary optimization variables $\beta_k[n]$ and $\mu_k'[n]$, we can bound the SINR. Consequently, C2 is equivalently replaced by the following constraints

$$\widehat{\text{C2a}}: \text{Tr}\big(\mathbf{W}_k[n]\tilde{\mathbf{H}}_k[n]\big) \geqslant \mu_k'[n]\beta_k[n], \tag{15}$$

$$\widehat{\text{C2b}}: \sum_{i\neq k}\text{Tr}\big(\mathbf{W}_i[n]\tilde{\mathbf{H}}_k[n]\big) + \sigma_k^2 s_k[n] \leqslant \beta_k[n], \tag{16}$$

where $\tilde{\mathbf{H}}_k[n] = \beta_0^2\mathbf{A}(\mathbf{q}[n], \mathbf{d}_k)$, and $\mathbf{A}(\mathbf{q}[n], \mathbf{d}_k) = \mathbf{a}(\mathbf{q}[n], \mathbf{d}_k)\mathbf{a}^H(\mathbf{q}[n], \mathbf{d}_k)$. The right-hand side of (15) is not a convex function. Similarly as in (11), by adopting the first-order Taylor approximation we obtain a convex function as $\chi_k[n] \triangleq 0.5\big(\mu_k'[n] + \beta_k[n]\big)^2 - \mu_k'^{(t)}\big(\mu_k'[n] - \mu_k'^{(t)}[n]\big) - \beta_k^{(t)}[n]\big(\beta_k[n] - \beta_k^{(t)}[n]\big)$. The left-hand side of (15) is also a non-concave function in trajectory $\mathbf{q}[n]$. Nevertheless, we can rewrite the left-hand side of (15) as

$$\text{Tr}\big(\mathbf{W}_k[n]\mathbf{H}_k[n]\big) = \beta_0^2\sum_{m=1}^{M}\sum_{m'=1}^{M}\mathbf{W}_{m,m'}^k[n]e^{\frac{j2\pi\frac{\hat{d}}{\lambda}H(m'-m)}{s_k[n]}}$$

$$= \underbrace{\beta_0^2\sum_{m=1}^{M}\mathbf{W}_{m,m}^k[n]}_{\triangleq U_k[n](\mathbf{W}_k)} + \beta_0^2\sum_{m=1}^{M}\sum_{m'=m+1}^{M}|\mathbf{W}_{m,m'}^k[n]|$$

$$\cos\left(2\pi\frac{\hat{d}}{\lambda}(m'-m)\frac{H}{\sqrt{s_k[n]}} + \phi_{m,m'}^{W_k}[n]\right) \triangleq J_k[n](\mathbf{W}_k, s_k), \tag{17}$$

where $\mathbf{W}^k_{m,m'}[n]$, is the element in the m^{th} row and m'^{th} column of $\mathbf{W}_k[n]$. Besides, $|\mathbf{W}^k_{m,m'}[n]|$ and $\phi^{W_k}_{m,m'}[n]$ denote the magnitude and phase of $\mathbf{W}^k_{m,m'}[n]$, respectively. Note that since the right-hand side of (15) is convex, we need to find an affine approximation of $J_k[n]$ to convexify the underlying optimization problem which is obtained by a first-order Taylor series as follows

$$\tilde{J}_k[n](\mathbf{W}_k, s_k) \triangleq J_k^{(t)}[n](\mathbf{W}_k, s_k) + \nabla_{J_k[n]}\big(s_k[n] - s_k^{(t)}[n]\big), \tag{18}$$

where (t) denotes the SCA iteration index and $\nabla_{J_k[n]}$ is given by

$$\nabla_{J_k[n]} = \frac{-2\beta_0^2\pi\hat{d}H(m'-m)}{\lambda\big(s_k^{(t')}[n]\big)^{\frac{3}{2}}} \sum_{m=1}^{M}\sum_{m'=m+1}^{M} |\mathbf{W}^k_{m,m'}[n]|$$
$$\sin\left(2\pi\frac{\hat{d}}{\lambda}(m'-m)\frac{H}{\sqrt{s_k^{(t')}[n]}} + \phi^{W_k}_{m,m'}[n]\right). \tag{19}$$

By substituting (18), (15) can be restated as follows

$$\widehat{\text{C2a}}: \; U_k[n](\mathbf{W}_k) + \tilde{J}_k[n](\mathbf{W}_k, s_k) \geqslant \chi_k[n]. \tag{20}$$

Similarly, the left-hand side of (16) can be approximated by its first-order Taylor series. As a result, the inequality in (16) can be restated as

$$\widehat{\text{C2b}}: \sum_{i\neq k}\big(U_i[n](\mathbf{W}_i) + \tilde{J}_i[n](\mathbf{W}_i, s_k)\big) + \sigma_k^2 s_k[n] \leqslant \beta_k[n]. \tag{21}$$

Finally, we deal with the non-convexity of the power consumption when the UAV moves. To do so, we introduce the auxiliary variable $y[n] \geqslant 0$, such that

$$y^2[n] = \sqrt{1 + \frac{\|\mathbf{v}[n]\|^4}{4v_0^4}} - \frac{\|\mathbf{v}[n]\|^2}{2v_0^2}, \tag{22}$$

which can be rewritten as

$$\frac{1}{y^2[n]} = y^2[n] + \frac{\|\mathbf{v}[n]\|^2}{v_0^2}. \tag{23}$$

Consequently, the second term in the power consumption during UAV flight can be restated as $P_i\big(y(n)-1\big)$. Hence, the power consumption during UAV flight can be restated as $\tilde{P}_{\text{fly}}$=$P_o\left(\frac{3\|\mathbf{v}[n]\|^2}{\Omega^2 r^2}\right)+$ $P_i\big(y(n)-1\big) + \frac{1}{2}r_0\rho s A_{\text{r}}\|\mathbf{v}[n]\|^3$. With the above manipulations, the optimization problem can be written as

$$\begin{aligned}
\mathcal{P}_3: \min_{\mathbf{q},\mathbf{v},s_k,y,\mu_k',\beta_k} \ & \mathcal{F} \triangleq \frac{1}{N}\sum_{n=1}^{N}\Bigg(\sum_{e=1}^{E}\alpha_{e,n}P_{\text{hover}}[n]+ \\
& (1-\sum_{e=1}^{E}\alpha_{e,n})\tilde{P}_{\text{fly}}(\mathbf{v}[n])\Bigg) \\
\text{s.t.} \ \ & \text{C17}: \frac{1}{y^2[n]} \leqslant y^2[n] + \frac{\|\mathbf{v}[n]\|^2}{v_0^2}, \\
& \text{C18}: s_k[n] \leqslant \|\mathbf{q}[n]-\mathbf{d}_k\|^2, \\
& \text{C2c}: \frac{1}{N}\sum_{n=1}^{N}\log_2(1+\mu_k'[n]) \geqslant R_{\min}^k, \forall k, \\
& \widehat{\text{C2a}}, \widehat{\text{C2b}}, \text{C7}-\text{C10}.
\end{aligned} \tag{24}$$

Problem $\mathcal{P}_3$ is still non-convex due to non-convex constraints C17 and C18. However, these constraints can be effectively handled with the SCA technique by deriving corresponding global lower bounds at a given local point. As a result, via applying the first-order Taylor expansion of the right-hand side of C17, the following global lower bound can be obtained: $y^2[n] + \frac{\|\mathbf{v}[n]\|^2}{v_0^2} \geqslant y^{(t)2}[n] + \frac{\|\mathbf{v}^{(t)}[n]\|^2}{v_0^2} + 2y^{(t)}[n](y[n]-y^{(t)}[n]) + \frac{2\mathbf{v}^{(t)}[n]}{v_0^2}(\mathbf{v}[n]-\mathbf{v}^{(t)}[n]) \triangleq g(y[n],\mathbf{v}[n])$, where $y^{(t)}[n]$ and $\mathbf{v}^{(t)}[n]$ are the values obtained in the t-th iteration of SCA. Besides, since $\|\mathbf{q}[n]-\mathbf{d}_k\|^2$ is a convex function with respect to $\mathbf{q}[n]$, we obtain the global lower bound based on the first-order Taylor expansion at the given point $\mathbf{q}^{(t)}[n]$ as $\|\mathbf{q}[n]-\mathbf{d}_k\|^2 \geqslant \|\mathbf{q}^{(t)}[n]-\mathbf{d}_k\|^2 + 2(\mathbf{q}^{(t)}[n]-\mathbf{d}_k)^T(\mathbf{q}[n]-\mathbf{q}^{(t)}[n]) \triangleq f(\mathbf{q}[n],\mathbf{d}_k)$. This leads to the following convex optimization problem

$$\begin{aligned}
\mathcal{P}_4: \min_{\mathbf{q},\mathbf{v},s_k,y,\mu_k',\beta_k} \ & \mathcal{F} \\
\text{s.t.} \ \ & \widetilde{\text{C17}}: \frac{1}{y^2[n]} \leqslant g(y[n],\mathbf{v}[n]), \\
& \widetilde{\text{C18}}: s_k[n] \leqslant f(\mathbf{q}[n],\mathbf{d}_k), \\
& \text{C2c}, \widehat{\text{C2a}}, \widehat{\text{C2b}}, \text{C7}-\text{C10}.
\end{aligned} \tag{25}$$

In each iteration t, we update the solution set and efficiently solve $\mathcal{P}_4$ by CVX. The proposed solution based on AO is summarized in **Algorithm 1**. Note that for sufficiently large penalty factors τ in $\mathcal{P}_2$, the objective function of $\mathcal{P}_1$ is non-increasing in each iteration of **Algorithm 1** and converges to a suboptimal solution with polynomial time computational complexity [18].

V. Simulation Results

In this section, we evaluate the performance of our proposed algorithm via computer simulation. We consider an area of 0.5 km $\times$ 0.5 km with $K = 2$ communication users and $E = 2$

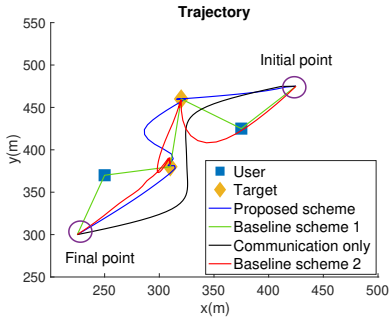

(a) UAV trajectories.

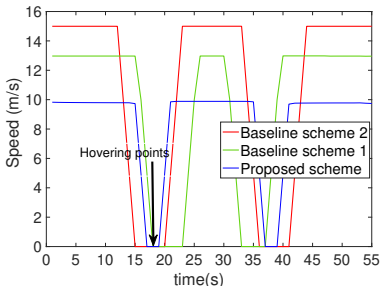

(b) Velocity of the UAV versus time (s).

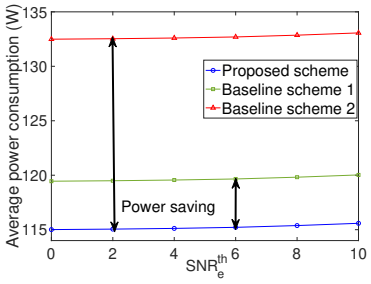

(c) Average power consumption versus the minimum required sensing SNR.

Fig. 3: Trajectory, velocity, and average power consumption of the UAV.

sensing targets. The UAV is equipped with $M = 6$ antennas and the minimum long-term sensing SNR at the UAV is $\text{SNR}_e^{\text{th}} = 0$ dB [9]. Moreover, the maximum flight speed of the UAV is $v_{\max} = 15$ m/s and the flight altitude is $H = 40$ m. Besides, the channel power gain at reference distance $d_0 = 1$ m is $\beta_0 = -30$ dB. Unless specified otherwise, we set $\sigma_e^2 = \sigma_k^2 = -110$ dBm, $P_{\max} = 40$ dBm, $R_{\min} = 1$ bps/Hz, $a_{\max} = 5$ m/s^2, $T = 55$ s, $D = 5$ m, and $\delta_t = 1$ s. To investigate the power saving achieved by our proposed scheme, we compare it with two baseline schemes. For baseline scheme 1, we adopt a heuristic trajectory where the UAV visits each communication user and sensing target based on the minimum distance path while optimizing the downlink information and sensing beamformers, the sensing indicator, and the velocity. For baseline scheme 2, we adopt zero-forcing beamforming for information transmission and assume an additional beam for sensing. We further assume that the velocity is fixed, i.e., $v_{\max} = 15$ m/s, and omit C9. Then, we jointly optimize the sensing beam, sensing indicator, and trajectory based on a modified version of $\mathcal{P}_1$.

Fig. 3(a) and Fig. 3(b) depict the trajectory and velocity of the UAV during its mission. In particular, for the proposed scheme, the UAV starts flying from the initial point towards the

location of the first target while transmitting data to the communication users. During this time, the UAV also controls its velocity to minimize power consumption. Fig. 3(b) shows that, for the proposed algorithm, the UAV prefers a speed of around 10 m/s rather than the maximum speed since this speed minimizes the aerodynamic power consumption of the UAV. When approaching the first sensing target, the UAV gradually reduces its velocity to zero to be able to hover above the target. Next, the UAV flies towards the second target and senses it while hovering. Finally, the UAV flies towards the final point while supporting the communication users. It is interesting to observe that the trajectory of the UAV is curved. This is because in order to save power, the UAV tries to fly at the optimum velocity and as close as possible to the communication users. Fig. 3(a) also shows the trajectory of the UAV when there is no sensing requirement. In this case, in order to save power, the UAV prefers to fly between both users simultaneously to support them. From Fig. 3(b), we can observe that for baseline scheme 1, as the trajectory is not optimized, the UAV needs to fly with a higher velocity to complete its mission which leads to a higher transmit power consumption as can be observed in Fig. 3(c).

Fig. 3(c) shows the average power consumption versus the sensing SNR requirement. The UAV's average power consumption for the proposed scheme and the baseline schemes is monotonically nondecreasing with respect to the minimum SNR threshold for sensing. This is because to meet more stringent sensing requirements, the UAV needs to transmit with high power. Moreover, we can observe the impact of velocity and trajectory optimization on the power consumption of the UAV. In particular, the proposed scheme requires less power compared to baseline scheme 1, which employs a fixed trajectory, as the trajectory design introduces extra degrees of freedom. Moreover, baseline scheme 2 also consumes more power in comparison with the proposed scheme. In fact for baseline scheme 2, in addition to the fixed beamforming policy which leads to a higher transmit power, a considerable amount of aerodynamic power is consumed because of the fixed high UAV velocity.

VI. Conclusion

The joint resource allocation and trajectory design for a multi-user multi-target UAV-based ISAC system was studied in this paper. We formulated the algorithm design as an optimization problem for minimization of the total UAV power consumption while taking into account the QoS requirements of the users and sensing tasks. Specifically, for the sensing task, synthesizing a focused beam with small sidelobes, achieving a required accumulated sensing SNR, and enforcing

Algorithm 1 Proposed resource allocation framework.

1. Initialize $\mathbf{W}_k^{(t)}[n]$, $\alpha_{e,n}^{(t)}$, $\mathbf{v}^{(t)}[n]$, $\mathbf{q}^{(t)}[n]$, $\mu_k^{(t)}$, $\phi_k^{(t)}$, $\beta_k^{(t)}$, $\mu_k'^{(t)}$, $\tau \gg 1$, t (iteration index), ε_{AO}.

Repeat

2. Solve $\mathcal{P}_2$ for given $\mathbf{v}[n] = \mathbf{v}^{(t)}[n]$, $\mathbf{q}[n] = \mathbf{q}^{(t)}[n]$ and obtain $\mathbf{W}_k^{(t+1)}[n]$, and $\alpha_{e,n}^{(t+1)}$.
3. Solve $\mathcal{P}_4$ for given $\mathbf{W}_k[n] = \mathbf{W}_k^{(t+1)}[n]$, $\alpha_{e,n}^{(t+1)}$, and obtain $\mathbf{v}^{(t+1)}[n]$, $\mathbf{q}^{(t+1)}[n]$.
5. Set $t = t + 1$
6. **until** $\frac{\mathcal{O}^{(t)} - \mathcal{O}^{(t-1)}}{\mathcal{O}^{(t-1)}} \leqslant \varepsilon_{\text{AO}}$.

the UAV to hover above the target during sensing for improving the sensing performance were considered. A computationally-efficient AO-based algorithm was developed for handling the resulting non-convex MINLP to obtain a high-quality suboptimal solution. Simulation results revealed dramatic power savings enabled by the proposed scheme compared to two baseline schemes.

REFERENCES

[1] F. Liu, Y. Cui, C. Masouros, J. Xu, T. X. Han, Y. C. Eldar, and S. Buzzi, "Integrated sensing and communications: Toward dual-functional wireless networks for 6G and beyond," *IEEE J. Select. Areas Commun.*, vol. 40, no. 6, pp. 1728–1767, Jun. 2022.

[2] F. Liu, C. Masouros, A. Li, H. Sun, and L. Hanzo, "MU-MIMO communications with MIMO radar: From co-existence to joint transmission," *IEEE Trans. Wireless Commun.*, vol. 17, no. 4, pp. 2755–2770, Apr. 2018.

[3] X. Liu, T. Huang, N. Shlezinger, Y. Liu, J. Zhou, and Y. C. Eldar, "Joint transmit beamforming for multiuser MIMO communications and MIMO radar," *IEEE Trans. Signal Process.*, vol. 68, pp. 3929–3944, Jun. 2020.

[4] L. Gupta, R. Jain, and G. Vaszkun, "Survey of important issues in UAV communication networks," *IEEE Commun. Surveys Tuts.*, vol. 18, no. 2, pp. 1123–1152, Nov. 2015.

[5] D. Xu, Y. Sun, D. W. K. Ng, and R. Schober, "Multiuser MISO UAV communications in uncertain environments with no-fly zones: Robust trajectory and resource allocation design," *IEEE Trans. Commun.*, vol. 68, no. 5, pp. 3153–3172, May. 2020.

[6] Q. Wu *et al.*, "A comprehensive overview on 5G-and-beyond networks with UAVs: From communications to sensing and intelligence," *IEEE J. Select. Areas Commun.*, vol. 39, no. 10, pp. 2912–2945, Oct. 2021.

[7] Z. Lyu, G. Zhu, and J. Xu, "Joint maneuver and beamforming design for UAV-enabled integrated sensing and communication," *IEEE Trans. Wireless Commun.*, pp. 1–1, 2022.

[8] K. Meng, Q. Wu, S. Ma, W. Chen, and T. Q. S. Quek, "UAV trajectory and beamforming optimization for integrated periodic sensing and communication," *IEEE Wireless Commun. Letts.*, vol. 11, no. 6, pp. 1211–1215, Mar. 2022.

[9] K. Meng, Q. Wu, S. Ma, W. Chen, K. Wang, and J. Li, "Throughput maximization for UAV-enabled integrated periodic sensing and communication," *IEEE Trans. Wireless Commun.*, vol. 22, no. 1, pp. 671–687, Jan. 2023.

[10] Z. Wei, F. Liu, D. W. K. Ng, and R. Schober, "Safeguarding UAV networks through integrated sensing, jamming, and communications," in *Proc. IEEE ICASSP*, 2022, pp. 8737–8741.

[11] Y. Rong, R. Gutierrez, K. V. Mishra, and D. W. Bliss, "Noncontact vital sign detection with UAV-borne radars: An overview of recent advances," *IEEE Veh Technol. Mag.*, vol. 16, no. 3, pp. 118–128, Sep. 2021.

[12] W. Wang and W. Zhang, "Jittering effects analysis and beam training design for UAV millimeter wave communications," *IEEE Trans. Wireless Commun.*, vol. 21, no. 5, pp. 3131–3146, May. 2022.

[13] M. I. Skolnik, "Introduction to radar," *Radar Handbook*, vol. 2, p. 21, 1962.

[14] Y. Zeng, J. Xu, and R. Zhang, "Energy minimization for wireless communication with rotary-wing UAV," *IEEE Trans. Wireless Commun.*, vol. 18, no. 4, pp. 2329–2345, Apr. 2019.

[15] D. Xu, X. Yu, D. W. K. Ng, A. Schmeink, and R. Schober, "Robust and secure resource allocation for ISAC systems: A novel optimization framework for variable-length snapshots," *IEEE Trans. Commun.*, vol. 70, no. 12, pp. 8196–8214, Dec. 2022.

[16] A. Khalili, E. M. Monfared, S. Zargari, M. R. Javan, N. M. Yamchi, and E. A. Jorswieck, "Resource management for transmit power minimization in UAV-assisted RIS HetNets supported by dual connectivity," *IEEE Trans. Wireless Commun.*, vol. 21, no. 3, pp. 1806–1822, Mar. 2022.

[17] X. Yu, D. Xu, D. W. K. Ng, and R. Schober, "IRS-assisted green communication systems: Provable convergence and robust optimization," *IEEE Trans. Commun.*, vol. 69, no. 9, pp. 6313–6329, Sep. 2021.

[18] J. C. Bezdek and R. J. Hathaway, "Some notes on alternating optimization," in *AFSS Int. Conf. Fuzzy Systems*. Springer, 2002, pp. 288–300.